

Original Research Article

Anti-resorptive effects of cementocytes during orthodontic tooth movement

Yufei Xie¹⁻³, Ning Zhao^{1-3*}, Gang Shen¹⁻³

¹Department of Orthodontics, Ninth People's Hospital, Shanghai Jiao Tong University School of Medicine, ²Shanghai Key Laboratory of Stomatology & Shanghai Research Institute of Stomatology, ³National Clinical Research Center of Stomatology, Shanghai, China

*For correspondence: **Email:** zhaon1995@126.com

Sent for review: 29 August 2018

Revised accepted: 25 October 2018

Abstract

Purpose: To investigate the mechanism involved in the anti-resorptive effect of cementocytes during orthodontic tooth movement in mice and human specimens.

Methods: The morphology, molecular structure and biological expression of cellular cementum in mice and human samples were examined using hematoxylin and eosin staining, immuno-histochemical staining, scanning electron microscopy, and Raman spectroscopy. The expressions of osteoprotegerin (OPG), receptor activator of nuclear κ B ligand (RANKL) and sclerostin (SOST) encoding genes in cementocytes and alveolar bone osteocytes were evaluated by quantitative real-time polymerase chain reaction (qRT-PCR).

Results: Results demonstrated that cementocyte lacunae were larger and more irregular in shape than the regular ellipsoid osteocyte lacunae. The ratio of phosphate to amino acid was significantly lower in cellular cementum than that in alveolar bone and dentin. In mice, OPG/RANKL ratio was significantly higher in cementocytes (4.8 ± 0.37) than in alveolar bone osteocytes (0.17 ± 0.42) in natural state. In humans, OPG/RANKL ratio was 1.41 ± 0.07 in cementocytes and 0.71 ± 0.04 in alveolar bone osteocytes under natural conditions, and 37.69 ± 0.15 in cementocytes and 1.95 ± 0.83 in alveolar bone osteocytes applying fluid flow shear stress. Moreover, SOST was extremely low expressed under force application in cementocytes.

Conclusion: Under fluid flow shear stress, cementocytes stimulate the differentiation of osteoblasts and inhibit the activation of osteoclasts, showing greater potential for bone protection than alveolar bone osteocytes. Cementocytes might play an important role in preventing root resorption in the process of orthodontic tooth movement.

Keywords: Cementocytes, Bone protection, Microfluidic chip, Orthodontic tooth movement

This is an Open Access article that uses a funding model which does not charge readers or their institutions for access and distributed under the terms of the Creative Commons Attribution License (<http://creativecommons.org/licenses/by/4.0>) and the Budapest Open Access Initiative (<http://www.budapestopenaccessinitiative.org/read>), which permit unrestricted use, distribution, and reproduction in any medium, provided the original work is properly credited.

Tropical Journal of Pharmaceutical Research is indexed by Science Citation Index (SciSearch), Scopus, International Pharmaceutical Abstract, Chemical Abstracts, Embase, Index Copernicus, EBSCO, African Index Medicus, JournalSeek, Journal Citation Reports/Science Edition, Directory of Open Access Journals (DOAJ), African Journal Online, Bioline International, Open-J-Gate and Pharmacy Abstracts

INTRODUCTION

Cementocytes are a class of cells embedded in the nucleus of the apical region of cells. They are similar to osteocytes with respect to histology

and molecular biology [1]. It has been revealed that in addition to maintaining basic morphology of bone, osteocytes perceive and transduce mechanical signals, modify surrounding environments, and regulate bone metabolism

[2,3]. Cementum cells are larger than osteocytes in morphological aspects, arranged randomly, and are very few in lacunar under certain conditions [4]. These cells are also located in osteocyte-like lacunar-canalicular system which could provide the microenvironment for mechanical sensing and transduction. However, the function of cementum, cell biology and molecular biology characteristics of cementocytes remains largely unrevealed.

Microfluidic technology is widely used in simulating and building multi-control system parameters [5-7]. Cementum and bone tissues are relatively unitary tissue composed of cell components, mainly cementocytes and osteocytes in bone matrix lacunae. Thus, microfluidic models of cementum and bone tissue are easier to establish than other complex organs. Microfluidic chip technology is a convenient approach for research on cementum and bone tissue.

Osteoprotegerin (OPG) is a major cytokine which physiologically inhibits bone resorption and the differentiation and activation of osteoclasts. It also induces osteoclast apoptosis by inhibiting the effect of receptor activator of nuclear κ B ligand (RANKL). RANKL is the only cytokine that can directly induce osteoclast differentiation and development, and participate in the regulation of osteoclast function. The ratio of OPG to RANKL determines the maturation and functional status of osteoclasts [8-10]. Sclerostin (SOST) is a negative regulator of bone mass, it acts on surrounding osteoblasts through synaptic transmission to the bone surface, reducing osteogenic rates under stress stimulation [11]. It has been revealed that sclerostin, as a mechanosensitive protein, may be the link between the mechanical induction of bone cells and the regulation of bone formation [12].

In the present study, the micro-environment of cellular cementum was designed and fabricated using microfluidic chip. Moreover, the cellular and molecular biology character of the cementum and alveolar bone in mice and human specimens were investigated in order to study the anti-resorptive mechanisms of cementocytes during orthodontic tooth movement.

EXPERIMENTAL

Animals

Three-month-old male C57BL6/J mice were purchased from the Experimental Animal Center of Ninth People's Hospital of Shanghai Jiaotong University School of Medicine, and maintained

on a national standard rodent feed. The mice were kept in cages in a room maintained at 21 – 24 °C with a 12-h / 12-h light/dark cycle.

Human specimens

Human teeth and alveolar bone specimens were obtained from 16 patients from Ninth People's Hospital of Shanghai Jiaotong University School of Medicine. The specimens were stored in alpha-MEM medium as soon as the teeth were removed. The patients' teeth and alveolar bone specimens were divided into natural state group and forced group. Fluid flow shear stress was loaded on cellular cementum and alveolar bone in a microfluidic chip. This system was composed of syringe, elite syringe pump, chip, pressure sensor, development board and petri dishes. The bearing pressure in the flow chamber was monitored in real-time using Arduino 1.6.9 software.

Histological and immuno-histochemical analyses of mice

Tissue sections treated in natural state and fluid flow shear stress were fixed in 4 % paraformaldehyde for 24 h at 4 °C, and decalcified in 10 % EDTA. The samples were dehydrated and embedded in paraffin. Each block was cut into 5- μ m thick sections using a microtome. Then, the sections were processed for hematoxylin & eosin (H & E) and immuno-histochemical staining (IHC). The stained sections were examined under an optical microscope. For OPG, RANKL and sclerostin immuno-histochemical staining, paraffin was removed from sections by immersing in xylene, and the sections were thereafter dehydrated through a serial *alcohol gradient*. To inhibit endogenous peroxidase activity, the sections were incubated with 3 % H₂O₂ for 10 min. After washing thrice in distilled water, they were incubated with monoclonal anti-OPG antibody, monoclonal anti-RANKL antibody, and monoclonal anti-sclerostin antibody (Abcam, UK) for 12 h at 4 °C. Subsequently, the sections were incubated with secondary biotin-labeled anti-mouse/rabbit antibody (Abcam, UK) for 30 min. Blank control groups were treated with PBS instead of primary antibody. Positive expressions were visualized by reacting with 3, 3'-diaminobenzidine (Boster Biotechnology, China) for 1 min.

Examination of cellular cementum and alveolar bone of mice

Tissue sections were fixed in 4 % paraformaldehyde for 24 h at 4 °C and

dehydrated through a serial *alcohol gradient*. Then, the samples were embedded in methyl methacrylate and cut into 100- μ m thick sections using a hard tissue slicer. Cellular cementum and osteocytes of mice were examined under a scanning electron microscope (SEM, JEOL Co, Japan).

Quantitative real-time polymerase chain reaction (qRT-PCR)

Total RNA was extracted from the mice and human tissues using Trizol Reagent (TaKaRa, Japan) according to the manufacturer's instructions. Genomic DNAs were digested with DNase I (Fermentas, USA). The RNA quality and purity were assessed by agarose gel electrophoresis. The RNA was then reverse-transcribed to cDNA using the RevertAid First Strand cDNA Synthesis Kit (Thermo Fisher Scientific, USA) following the manufacturer's protocol. Real-time PCR amplification was carried out using AceQ qPCR SYBR Green Master Mix (Vazyme Biotech Co., China) in Thermal Cycler Dice Real Time System (Thermo Fisher Scientific, USA) for 2 min at 95 °C, and 40 cycles for 15 sec at 95 °C, 20 sec at 60 °C, and 20 sec at 72 °C. Specific PCR primers were designed according to the respective cDNA sequences (Table 1). The relative expressions were quantified using the $2^{-\Delta\Delta CT}$ method [13].

Ethical approval

This research was approved by the Animal Ethical Committee of Shanghai Jiao Tong University School of Medicine (approval no. A20180120) and carried out according to the guidelines of "Principles of Laboratory Animal Care" (NIH publication no. 85-23, revised 1985) [14].

The human studies were also approved by the Ethical Committee of Shanghai Jiao Tong

University School of Medicine (approval no. H20180120) and was carried out according to the guidelines of Declaration of Helsinki promulgated in 1964 as amended in 1996 [15].

Statistical analysis

All experimental data were analyzed using SPSS (version 21.0, IBM, USA). One-way analysis of variance was performed to determine differences between groups. $P < 0.05$ was considered to be statistically significant.

RESULTS

Outcome of H & E staining of cementum and alveolar bone in mice

The appearance of H & E-stained section of the mouse mandibular under the microscope is shown in Figure 1. The first molar revealed that the basophilic cellular cementum, dentin and alveolar bone were pale pink, while the nuclei were blue. Cellular dentition, bone tissue cellular cementum and alveolar bone were basically similar in staining. A thin layer structure appeared in the middle segment of the root and acellular cementum, and the apical area was completely composed of cell cementum.

Cementocytes located in the bone lacunae of cellular cementum were diverse and irregular in morphology i.e. round, oval or columnar. Nevertheless, the nuclei were round and located in the middle of the cells. Compared with surface cells, the deep cementocytes were smaller in size and more diverse in shape. Empty lacuna could be found in the deep cellular cementum. Pluralities of cells existed in the part of cementum lacunae, although this phenomenon was not observed in alveolar bone.

Table 1: Primers used for real-time PCR

Variable		Forward	Reverse
Mice	ACTIN	5'-GGCTGTATTCCCCTCCATCG-3'	5'-CCAGTTGGTAACAATGCCATGT-3'
	OPG	5'-TCAGAAAGGAAATGCAACACA-3'	5'-CCGTTTTATCCTCTCTACTACT-3'
	RANKL	5'-GCCTCCCGCTCCATGTTTC-3'	5'-TGGCCCTCCTGGGGCTGGG-3'
Human	ACTIN	5'-GCACCCAGCACAATGAAGA-3'	5'-AATAAAGCCATGCCAATCTCA-3'
	OPG	5'-CCTTGCCCTGACCACTACTACA-3'	5'-TTGCACCACTCCAAATCCAG-3'
	RANKL	5'-GTATGCCAACATTTGCTTTTCG-3'	5'-GCTTCCTCCTTTTCATCAGGGTA-3'
	SOST	5'-ATCATCCATTGGGGTAGAAAAG-3'	5'-CAGAAGGCGGTGTCTCAAAA-3'

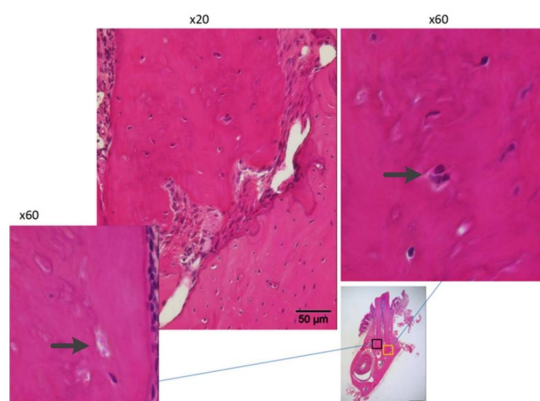


Figure 1: Representative photomicrographs of cementum and surrounding alveolar bone in mice

Outcome of immuno-histochemical staining of cementum and alveolar bone in mice

Bone sclerosis proteins were brown granules and were expressed in the cellular cementum and alveolar bone of mice. At high magnification, the cells of positive expression in the alveolar bone were more in number than those in the cellular cementum. Positive expressions of OPG and RANKL in the cellular cementum and alveolar bone appeared as *brownish-yellow* granules, but their expression levels differed slightly. The expression of OPG in cellular cementum was higher than that in alveolar bone, while the expression of RANKL in cellular cementum was slightly lower than that in alveolar bone (Figure 2). The negative control group was incubated with PBS instead of primary antibody. Thus, no positive expression was found there.

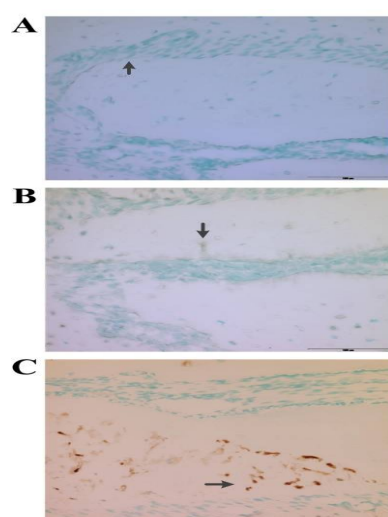


Figure 2: (A) Immunostaining image of cellular cementum and surrounding alveolar bone in mice OPG, (B) RANKL, (C) sclerostin. Positive products appear as brown particles

SEM images of cellular cementum and alveolar bone hard tissue sections

The SEM images showed that the morphology of lacunae in the bone cells was regular and mainly oval, but the lacunae in cementum cells were morphologically diverse and unevenly distributed in the matrix (Figure 3). After acid etching treatment, specimens embedded in resin clearly displayed cementocytes, alveolar bone and bone canaliculus under SEM. There were many lacunae in the cellular cementum, and the small tube from the lacuna was connected with that from the adjacent lacuna to form a reticular system. The distribution was uniform and the quantity was large for tubes in osteocytes of alveolar bone. However, compared with the bone tissue, the number was smaller and the shape was more irregular in cementum lacunae. The small tube from the lacuna was less numerous and shorter than that from cementum cells (Figure 4).

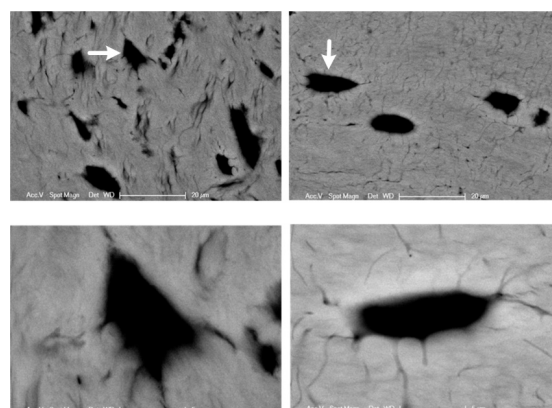


Figure 3: Backscattered SEM analysis of cellular cementum and alveolar bone

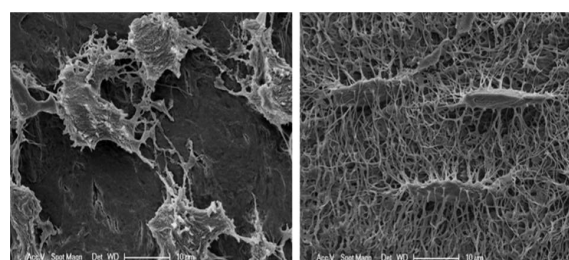


Figure 4: Acid-etching resin-embedded cellular cementum and alveolar bone in SEM

Acid-etching resin-embedded sample allowed visualization of resin-filled lacunae and canaliculi of cellular cementum and osteocytes

Expression of OPG and RANKL in cementocytes and alveolar bone osteocytes

In order to study the expression patterns of OPG and RANKL, real-time PCR was performed, with

β -actin as reference gene. In mice, the results demonstrated that the expression of OPG in cementocytes was significantly lower than that in alveolar bone osteocytes, and the OPG/RANKL ratio of the former was much higher than that of the latter. Using β -actin as reference, the expression of OPG in cementum cells was 1.67 ± 0.46 , which was higher than that in alveolar bone cells (1.15 ± 0.44) (Figure 5), although the difference was not statistically significant.

RANKL had an expression level of 0.34 ± 0.18 in cementocytes, which was significantly lower than that in alveolar bone osteocytes (6.63 ± 0.13). Correspondingly, the OPG/RANKL ratio in cementocytes was 4.8 ± 0.37 , which was significantly higher than that in alveolar bone osteocytes (0.17 ± 0.42).

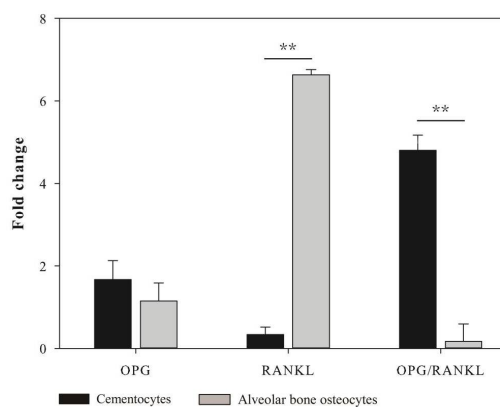


Figure 5: Expressions of OPG, RANKL and SOST in cementocytes and alveolar bone osteocytes under natural condition. Error bars represent standard deviation; ** $p < 0.01$

Effect of fluid shear stress on expressions of OPG, RANKL and SOST

Under natural condition, the OPG/RANKL ratio in cementocytes (1.41 ± 0.07) was significantly higher than that in alveolar bone osteocytes (0.71 ± 0.04) in humans (Figure 6C). The pattern of changes in expressions of OPG and RANKL was same as that in mice. The expression level of SOST in cementocytes was 0.60 ± 0.01 , while that in alveolar bone osteocytes was 1.00 ± 0.09 . However, no significant differences in the expressions of OPG, RANKL and SOST between cementocytes and alveolar bone osteocytes were observed.

To determine the effect of fluid shear stress on the expressions of OPG, RANKL and SOST, the expression patterns of these genes in human samples were analyzed by qRT-PCR using β -actin as reference gene. The results showed that the expression level of OPG in cementocytes

increased significantly, when compared to that under natural state (Figure 6 A). Due to fluid shear stress, the expression level of OPG increased from 0.71 ± 0.09 under natural condition to 2.76 ± 0.46 , corresponding to a 3.89-fold increase. In alveolar bone osteocytes, fluid shear stress up-regulated the expression of OPG and resulted in a fold change of 4.47.

Under fluid shear stress, the expression of RANKL in cementocytes decreased very appreciably to 0.03 ± 0.04 , but improved remarkably in alveolar bone osteocytes (1.41 ± 0.12) (Figure 6 B). From the expression profiles of OPG and RANKL, the ratio of OPG/RANKL in cementocytes was 37.69 ± 0.15 , which was significantly higher ($p < 0.01$) than that in alveolar bone osteocytes (1.95 ± 0.83) (Figure 6 C). In addition, the expression of SOST was inhibited in cementocytes. The expression level of this gene was down-regulated from 0.60 ± 0.01 to 0.08 ± 0.01 when subjected to fluid shear stress. However, the expression of SOST in the alveolar bone cell improved slightly (fold change = 1.39) under fluid shear stress (Figure 6 D).

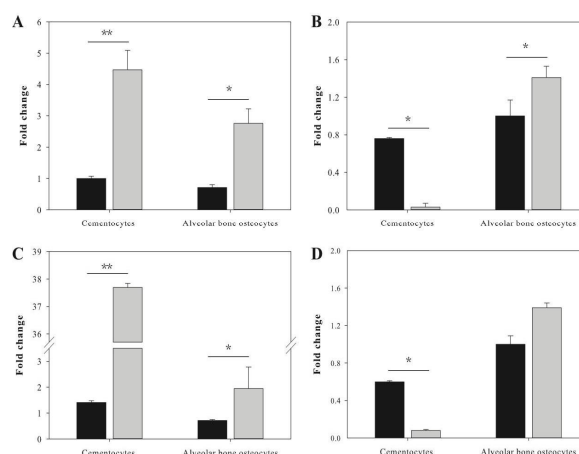


Figure 6: Expressions of OPG, RANKL and SOST in cementocytes and alveolar bone osteocytes under fluid flow shear stress. A: OPG, B: RANKL, C: OPG/RANKL, D: SOST. The error bars represent standard deviations; * $p < 0.05$, ** $p < 0.01$

DISCUSSION

Histological studies in mice revealed that the cell morphology of cementocytes was diverse (i.e. circular, oval or columnar) and empty lacuna were located in the deep cementum, relative to alveolar bone cells [1,4]. Pluralities of cells existed in some cementum lacunae, but were absent in alveolar bone. In addition, SEM examination showed that relative to osteocytes, alveolar bone protuberances was less and disordered, the tubules were less and shorter,

and the reticular system was loose and irregular in shape [16,17]. Lacunar tubules bury cell bodies, and the cell protrusions are interlinked to form a reticular system for communication and exchange of metabolites. Multiple cells are connected together through the gap junctions between the protrusions to form a multinucleated syncytium that allows cellular signals to pass between multiple cells [3,18].

Osteoprotegerin (OPG) is composed of osteoblasts or stromal cells. Its main function is to inhibit osteoclast differentiation and activation, and to induce osteoclast apoptosis by inhibiting RANKL. The latter is the only cytokine that can directly induce osteoclast differentiation and development, while participating in the regulation of osteoclast function. Its main function is to stimulate osteoclast differentiation and activation, and inhibit osteoclast apoptosis. Therefore, the ratio of OPG to RANKL determines the maturation and functional status of osteoclasts [2,19-21].

In the present study, immuno-histochemical staining showed that the positive expressions of OPG and RANKL occurred in the cementum and alveolar bone of mice, which revealed similarities between the two in bone remodeling function. The expression level of OPG and RANKL were slightly different between the two tissues. The expression of OPG was higher in cementum than in alveolar bone, while the expression of RANKL was low in cementum and high in alveolar bone. Compared with osteocytes, cementocytes have the potential to promote osteogenesis and inhibit osteoclasts. This may account for much higher levels of alveolar bone remodeling than root surface remodeling during orthodontic tooth movement. Studies have demonstrated that during orthodontic tooth movement, the OPG/RANKL system plays an important role in the resorption and remodeling of alveolar bone [22-24].

Under natural condition, the OPG/RANKL ratio in alveolar bone is relatively constant. However the ratio changes under the influence of an external force, resulting in the regulation of osteoclast differentiation and function, with effects on alveolar bone remodeling. The results of the present study reveal that the expressions of OPG and RANKL were increased under fluid shear stress, but the changes in OPG were more obvious. Under fluid shear stress, alveolar osteoclasts were active, but OPG bound to RANKL competitively inhibited osteoclastic bone resorption, thereby regulating the dynamic balance between bone resorption and bone formation. This suggests that OPG maintains a

stability in the balance between osteoblasts and osteoclasts, thus preventing the absorption of alveolar bone and cementum.

OPG/RANKL ratio was higher in cementocytes than in alveolar bone under natural conditions. Fluid shear stress promoted OPG expression but inhibited RANKL expression, which led to the significant increase in OPG/RANKL ratio. This implies that cementocytes inhibit differentiation and activation of osteoclasts under non-stress conditions. Thus, stress stimulation further strengthened this effect, showing significant potential for bone protection in humans.

SOST gene is mainly expressed in bone cells and encodes sclerostin. Sclerostin is secreted by mature bone cells, and is transmitted to the bone surface through the synapse under stress stimulation. It acts on osteoblasts and reduces the rate of osteogenic. Sclerostin and SOST gene are expressed in human and mice cementocytes [25,26]. Studies have shown that sclerostin inhibits the formation of cementum by inhibiting mineralization-related genes. At the same time, sclerostin acts on the OPG/RANKL system which is related to the root resorption process [27]. Moreover, sclerostin and the SOST gene have high expression levels in cementocytes. It has been reported that the expression of IDG-CM6 in cementum cell line also appeared certain phase, so SOST might be related to the repair of cementum [1].

The results from human samples revealed that both cementum and alveolar bone cells expressed SOST, and there was no significant difference between them in natural state. However, under fluid shear stress, SOST levels decreased significantly in cementum. Two hours later, the cementum responded to the mechanical stimulation and promoted activation of bone remodeling. Compared with the alveolar bone, the gene expressions of the negative regulator of osteogenesis were lower in cementum. This is beneficial for maintenance of the balance between osteogenesis and osteoclasts. Thus, the cementum may play an important role in preventing root resorption during orthodontic tooth movement.

CONCLUSION

Cementocytes in cellular cementum and osteocytes in alveolar bone have a certain similarity in histomorphology. Under fluid flow shear stress, cementocytes stimulate the differentiation of osteoblasts and inhibit the activation of osteoclasts, showing greater

potential for bone protection than alveolar bone osteocytes.

DECLARATIONS

Acknowledgement

This study was supported by the Shanghai JiaoTong University Degree Project: Research on the Protective Effects of Cementocyte SOST Gene against Tooth Root Resorption during Orthodontic Tooth Movement, and Shanghai Jiao Tong University Medical-Engineering Cross Project: Research on the Establishment of Cementum Organ Chip and Its Bone Remodelling Effects on the Periodontium (grant no. YG2016MC06).

Conflict of interest

The authors declare that no conflict of interest is associated with this work.

Contribution of authors

This work was done by the authors named in this article and the authors accept all liabilities resulting from claims which relate to this article and its contents. The study was conceived and designed by Ning Zhao and Gang Shen; Yufei Xie, Ning Zhao and Gang Shen collected and analysed the data while Yufei Xie wrote the text. All authors read and approved the text prior to publication.

REFERENCES

1. Ayasaka N, Kondo T, Goto T, Kido M, Nagata E, Tanaka T. Differences in the transport systems between cementocytes and osteocytes in rats using microperoxidase as a tracer. *Arch Oral Biol* 1992; 37(5): 363-369.
2. Bonewald LF. The amazing osteocyte. *J Bone Miner Res* 2011; 26(2): 229-238.
3. Dallas SL, Prideaux M, Bonewald LF. The osteocyte: an endocrine cell and more. *Endocr Rev* 2013; 34(5): 658-690.
4. Zhao N, Foster B, Bonewald L. The Cementocyte-An Osteocyte Relative? *J Dent Res* 2016; 95(7): 734-741.
5. Holt WV, Pickard AR. Role of reproductive technologies and genetic resource banks in animal conservation. *Rev Reprod* 1999; 4(3): 143-150.
6. Huh D, Kim HJ, Fraser JP, Shea DE, Khan M, Bahinski A, Ingber DE. Microfabrication of human organs-on-chips. *Nat Protoc* 2013; 8(11): 2135-2157.
7. Whitesides GM. The origins and the future of microfluidics. *Nat* 2006; 442(7101): 368-373.
8. Aoyama E, Kubota S, Khattab HM, Nishida T, Takigawa M. CCN2 enhances RANKL-induced osteoclast differentiation via direct binding to RANK and OPG. *Bone* 2015; 73: 242-248.
9. Roberts WE, Epker BN, Burr DB, Hartsfield JK, Roberts JA. Remodeling of mineralized tissues, part II: control and pathophysiology. *Semin Orthod* 2015; 12(4): 238-253.
10. Roberts WE, Roberts JA, Epker BN, Burr DB, Hartsfield JK. Remodeling of mineralized tissues, part I: the frost legacy. *Semin Orthod* 2006; 12(4): 216-237.
11. Poole KE, van Bezooijen RL, Loveridge N, Hamersma H, Papapoulos SE, Löwik CW, Reeve J. Sclerostin is a delayed secreted product of osteocytes that inhibits bone formation. *FASEB J* 2005; 19(13): 1842-1844.
12. Balemans W, VanHul W. Human genetics of SOST. *J Musculoskelet Neuronal Interact* 2006; 6(4): 355.
13. Livak KJ, Schmittgen TD. Analysis of relative gene expression data using real-time quantitative PCR and the 2- $\Delta\Delta CT$ method. *Methods* 2001; 25(4): 402-408.
14. World Health Organization. Principles of laboratory animal care. *WHO Chron* 1985; 39: 51-56.
15. World Health Organization. Declaration of Helsinki. *Br Med J* 1996; 313(7070): 1448-1449.
16. Kagayama M, Sasano Y, Mizoguchi I, Takahashi I. Confocal microscopy of cementocytes and their lacunae and canaliculi in rat molars. *Anat Embryol* 1997; 195(6): 491-496.
17. Scivetti M, Pilolli GP, Corsalini M, Lucchese A, Favia G. Confocal laser scanning microscopy of human cementocytes: analysis of three-dimensional image reconstruction. *Ann Anat* 2007; 189(2): 169-174.
18. Bosshardt D, Schroeder HE. Evidence for rapid multipolar and slow unipolar production of human cellular and acellular cementum matrix with intrinsic fibers. *J Clin Periodontol* 1990; 17(9): 663-668.
19. Ben-awadh AN, Delgado-Calle J, Tu X, Kuhlenschmidt K, Allen MR, Plotkin LI, Bellido T. Parathyroid hormone receptor signaling induces bone resorption in the adult skeleton by directly regulating the RANKL gene in osteocytes. *Endocrinol* 2014; 155(8): 2797-2809.
20. Nakashima T, Hayashi M, Fukunaga T, Kurata K, Oh-hora M, Feng JQ, Wagner EF. Evidence for osteocyte regulation of bone homeostasis through RANKL expression. *Nat Med* 2011; 17(10): 1231-1234.
21. Zhao S, Kato Y, Zhang Y, Harris S, Ahuja S, Bonewald L. MLO-Y4 osteocyte-like cells support osteoclast formation and activation. *J Bone Miner Res* 2002; 17(11): 2068-2079.
22. Khosla S. Minireview: The OPG/RANKL/RANK system. *Endocrinol* 2001; 142(12): 5050-5055.
23. Kong YY, Boyle WJ, Penninger JM. Osteoprotegerin ligand: a common link between osteoclastogenesis, lymph node formation and lymphocyte development. *Immunol Cell Biol* 1999; 77(2): 188-193.
24. Simonet W, Lacey D, Dunstan C, Kelley M, Chang MS, Lüthy R, Boone T. Osteoprotegerin: a novel secreted

- protein involved in the regulation of bone density. *Cell* 1997; 89(2): 309-319.
25. Jäger A, Götz W, Lossdörfer S, Rat-Deschner B. Localization of SOST/sclerostin in cementocytes in vivo and in mineralizing periodontal ligament cells in vitro. *J Periodontal Res* 2010; 45(2): 246-254.
26. Lehnen SD, Götz W, Baxmann M, Jäger A. Immunohistochemical evidence for sclerostin during cementogenesis in mice. *Anna Anat Anatomischer Anz* 2012; 194(5): 415-421.
27. Bao X, Liu Y, Han G, Zuo Z, Hu M. The effect on proliferation and differentiation of cementoblast by using sclerostin as inhibitor. *Int J Mol Sci* 2013; 14(10): 21140-21152.